

# Visual Recognition of the Initial and End Points of Lap Joint for Welding Robots

Prasarn Kiddee

*The State Key Laboratory of Management and  
Control for Complex Systems  
Institute of Automation  
Chinese Academy of Sciences  
Beijing, China, 100190  
prasarnkid@gmail.com*

Zaojun Fang and Min Tan

*The State Key Laboratory of Management and  
Control for Complex Systems  
Institute of Automation  
Chinese Academy of Sciences  
Beijing, China, 100190  
fzaoj@163.com, tan@compsys.ia.ac.cn*

**Abstract**—This paper describes a recognition method for the initial and end points of lap joints based on the image processing techniques. The edge detection technique is used in order to find the edges of the image. And the image processing techniques are employed in order to link the broken edges and find T-junctions of the image which are determined as candidates for the initial and end points of the weld seam. The T-junctions that match the conditions of angles checking and coordinate comparing will be detected as initial and end points of weld seam. The proposed method mainly insists of the 4 steps namely 1) smoothing the image and extracting edges of the image by using Canny operator 2) linking broken edges 3) detecting T-junctions and 4) analysing the initial and end points of weld seams. The experimental results showed that the initial and end points of the lap joints can be precisely recognized using the methods proposed in this paper.

**Index Terms**—lap joint welding, initial and end points, Canny operator, linking process, T-junction, angles checking, coordinate comparison, welding robot system.

## I. INTRODUCTION

In the autonomous welding control system, there are three key components which are: 1) welding parameter control; 2) welding robot control; and 3) weld seam detection. The research on welding parameter control is widely studied for decades. The results of these researches have been fully implemented in welding industries. The control technology on welding robots has also been studied and developed progressively. Nowadays, welding robots are not only used in large factories but also in small workshops [1]. Moreover, the shapes and positions of weld seams change frequently, which requires that the robot can detect the welding seams autonomously. However, because of the complexities of welding pieces and environments, it seems that the development in this area has many difficulties and needs to be more studied. In welding recognition system, the detection of the initial and end points for weld seams is a crucial factor. The accuracy of the detection of the two points directly have influence on the welding quality. For this reason, the development of precise detection of the initial and end points is essentially required in autonomous welding. Some researchers have

studied the problem of visual detection of the two points for welding robots. Zaojun F. et al, [2] proposed the initial weld point positioning method for container manufacturing which has two weld seams. The method composed of two main steps, i.e., computing the image feature and parameters of the seam line and computing the target image feature of seam line based on geometric relationship and aligning torch based on the difference between the target and current image features. Wei S. et al, [3] used morphological corrosion edge detection algorithm to extract the weld seam and boundaries. Then Hough transform was utilized as line detector. The intersection point of the weld seam line and boundary line was considered as the initial welding position. M. Kong et al, [4] described how to use Harris corner detector to find the initial position of the seam for welding robot in global environment. A potential couple of corners which had three distributing directions of the contour in the local area were detected as the initial position of the seam. Xizhang et al, [5] introduced template matching and polynomial interpolation technology of pixel to locate the initial weld position on aluminum work-piece. Furthermore, the initial position was transformed to real world coordinate system. The above researches on the detection of the initial and end points are only applied to the weld seam in butt joint welding. As to its simple geometry, weld seam of butt joint can be easily observed from any angle of views. Unlike butt joint, lap joint is formed by overlapping of two plates, thus its geometry will be more complex than butt joint. And we cannot capture the image of weld seam of lap joint from back and top view. For this reason, in lap joint welding, we must set camera toward the weld seam. Another problem is that there is shadow around the seam of lap joint which will lead to difficulty of image processing.

In this study, we employ Canny operator to detect the edge of the weld image. Then linking process is applied to the broken edges and line points. Template match method is used to find T-junctions which are considered as candidates for initial and end points. Finally, angle checking and coordinate

comparison are used to select the true initial and end points of the lap joint. Experiments are fully conducted to verify effectiveness of the proposed method in this paper.

## II. IMAGE PREPROCESSING AND EDGE EXTRACTION

### A. Image Preprocessing

The captured image contains much noise. Therefore, in the first step, noise reduction is applied to the image to improve the image quality. In this paper, the 2D Gaussian filter is used as the noise remover. The Gaussian filter function is

$$G(x, y) = \frac{1}{\sqrt{2\pi\sigma^2}} e^{-\frac{(x^2+y^2)}{2\sigma^2}} \quad (1)$$

where  $\sigma$  is standard deviation of distribution,  $x$  and  $y$  are random variable in 2-dimensional space. Fig. 1 shows original gray scale image, smoothed image, and Gaussian kernel respectively.



(a) Original image



(b) Smoothed image

$$\frac{1}{159} \times \begin{bmatrix} 2 & 4 & 5 & 4 & 2 \\ 4 & 9 & 12 & 9 & 4 \\ 5 & 12 & 15 & 12 & 5 \\ 4 & 9 & 12 & 9 & 4 \\ 2 & 4 & 5 & 4 & 2 \end{bmatrix}$$

(c) 5×5 Gaussian kernel

Fig. 1 The images and kernel in the image preprocessing stage

### B. Edge Extraction

Edge detection plays important role in image processing. The impeccable edge extraction indicates the quality of image

processing. In this paper, Canny edge detector is employed, which is divided into three steps as described below.

1) *Gradient magnitudes and directions computation*: In this step we will find the edge strength by taking the gradient of the smoothed image. For a function  $f(x, y)$ , the gradient of  $f$  at coordinate  $(x, y)$  can be defined as

$$\nabla f = \begin{bmatrix} G_x \\ G_y \end{bmatrix} \quad (2)$$

where  $G_x, G_y$  is the gradient magnitude in  $x$  and  $y$  direction respectively. Then the gradient magnitude of pixel at  $(x, y)$  is given by equation (3). And the direction of the gradient of the pixel can be computed by using equation (4).

$$mag(\nabla f) = [G_x^2 + G_y^2]^{\frac{1}{2}} \quad (3)$$

$$\theta = \tan^{-1} \left( \frac{G_y}{G_x} \right) \quad (4)$$

To estimate the gradient magnitude in practice, the Sobel operator is implemented. The Sobel operator performs as 2-D spatial gradient measurement on an image [6]. The Sobel operator uses a pair of 3×3 convolution kernel, shown in Fig. 2, one estimating the gradient in the  $x$ -direction and the other estimating the gradient in the  $y$ -direction.

-1	-2	-1
0	0	0
1	2	1

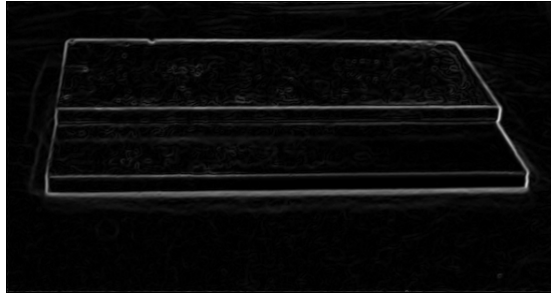
-1	0	1
-2	0	2
-1	0	1

Fig. 2 Sobel kernel for  $x$ -direction and  $y$ -direction

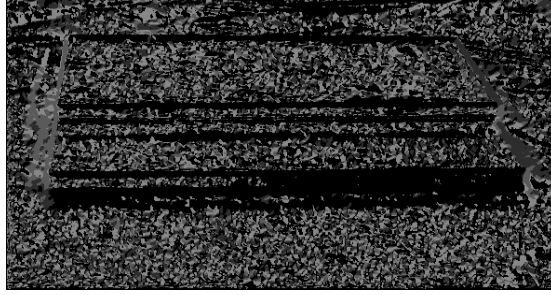
By using this operator, the approximate absolute gradient magnitude at each pixel can be estimated. Fig.3 shows the gradient magnitude image and gradient direction image respectively.

2) *Non-maxima suppression*: After the edge directions are known, non-maximum suppression is applied to the gradient magnitude image. The 8-connected neighborhood is used to trace along the edge in each edge direction and suppress the pixels that are not considered to be in an edge. This results a thin line in the output image. The output of non-maxima suppression is shown in Fig. 4.

3) *Double Threshold and Edge Tracing*: In this step, we use two thresholds, a high (T-high) and a low (T-low), to classify the strength of the edges. Any pixel in the image that has a value greater than T-high is presumed to be a strong edge pixel, and it is marked as a real edge pixel. Then, any pixel that connects to a strong edge pixel and that has a value greater than T-low is also selected as a real edge pixel. And the rest pixels that have value lower than T-low will be eliminated. The results of edge detection for lap point weld plate is shown in Fig. 5.



(a) Gradient magnitude image



(b) Gradient direction image

Fig. 3 The gradient magnitude and direction image

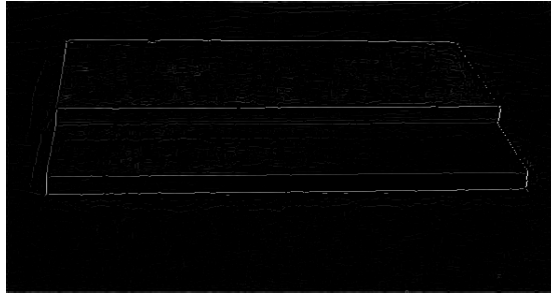


Fig. 4 The output of non-maximum suppression

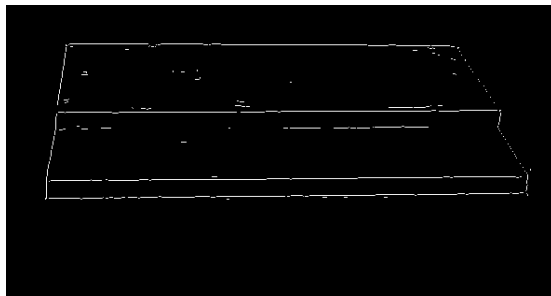


Fig. 5 The output of Canny edge detection

### III. LINKING PROCESS

According to the results of Canny edge detection, broken edges, line points, noisy edges and points exist in the image. Thus, noisy edges and points should be removed, and broken edges should be linked accordingly. Generally, there are two assumption about edge linking, i.e., 1) true edges or line

points in the image follow continuity patterns, whereas the false ones do not follow any such continuity, 2) the strength at edges or line pixels are greater than those at false edges [8]. In our study, the linking process is based on this assumption as described below.

4) *Noisy edges and points removing*: In first step, noisy edge are removed by using a threshold which is assigned by the length and shapes of noisy edge. Then, we apply  $13 \times 13$  square patch to every pixel in the image to find the line points. If a point was detect as a single one (no neighbor pixel), it will be marked as a noisy point and eliminated.

5) *End points detection and line points grouping*: From previous step, we have edge segments and line points in the image. In order to link the edge segments, the end points of each edge segment should be located by using 8-connected neighborhood. The line points should be classified using the slope between two line points. As shown in equation (5), if the difference of slope at  $i$  and  $i+1$  end point is greater than a threshold value, it implies that they are not on the same edge.

$$|m_{i+1} - m_i| \leq st \quad (5)$$

where  $m_i$  is the slope between two points,  $st$  is a slope threshold.

6) *Line points linking*: In case of straight edge, one of the simplest and applicable approaches to link line points is to analyze the strength of the gradient magnitude between the edge pixels. Firstly, we set the rectangular area between two line points in edge image as shown in Fig. 6. Then, at the same area of edge image, the gradient magnitude of each pixel in the same row will be compared. The position of the strongest gradient magnitude pixel will be recorded in order to be used as edge pixel position in the edge image. Finally, the pixel at the recorded position in the edge image will be changed to edge pixel. This process is applied to every line point in the edge image and the results are shown in Fig. 7.

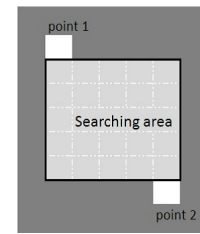


Fig. 6 Illustration of Line points linking concept

7) *Straight edges linking*: The edge segments in the vertical direction will be firstly linked. The  $3 \times 3$  patch is used to check the directions at the end of edge segment. If other end point of the edge segment is detected, these two end points of edge segments will be linked. Otherwise it will be marked as a corner pixel. For the horizontal edge segments,

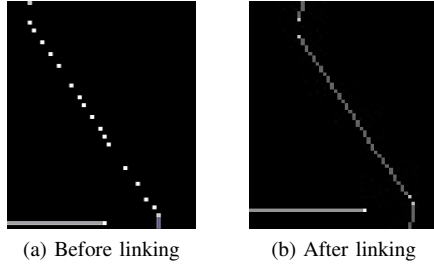


Fig. 7 The result of line points linking procedure

we apply the same process as explained above. Next, we will link horizontal and vertical edge segments together. By using  $3 \times 3$  patch, the end points of horizontal edge segments and their directions are detected. We use these end points as the starting points for  $3 \times 3$  patch. And the patch is set to move in detected direction to find the pixels of vertical edge segments. If the edge pixels of vertical segment are found in the gap between the starting point and detected point will be filled. Otherwise, this points will be marked as a corner pixel.

8) *Non-straight edges linking*: The edge segments at corner areas are not straight line. Thus the linking procedures for line points is employed. The flow chart of linking process is shown in Fig. 8. And Fig. 9 shows the results of linking process.

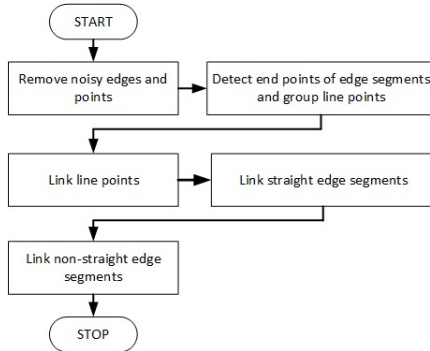


Fig. 8 The flow chart of linking process

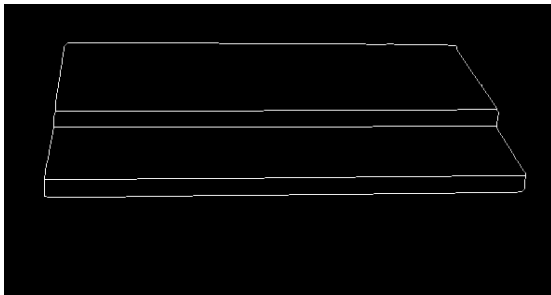


Fig. 9 The final result of linking process

#### IV. INITIAL AND END POINT DECISION

In the previous section, the proper edge segments are obtained. In this section, T-junctions which will be used as candidates for the initial and end points of lap joint in the image will be detected and analyzed.

##### A. T-junction Detection

T-junction in the image has basic forms as shown in Fig.10. Thus their locations can be detected easily by using  $3 \times 3$  patch in the image. When the T-junction is detected, the coordinate of each T-junctions will be recorded in order to be used in the next step. Fig.11 shows the results of T-junction detection.

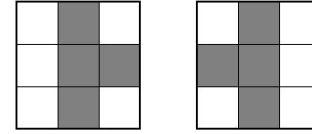


Fig. 10 The basic forms of T-junction

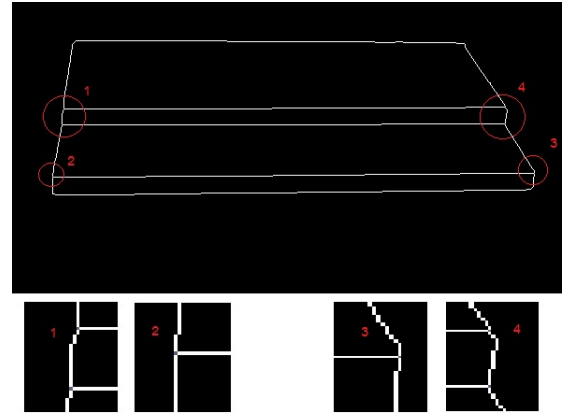


Fig. 11 The result of T-junction detection

##### B. Initial and End point Decision

In this step, the angles of T-junction will be computed and analyzed.

1) *Angles computation*: Firstly, the distance and the angles between the edge pixel at the center of T-junction and the edge pixels at designated positions is calculated. As shown in Fig.12,  $(x_0, y_0)$  is the coordinate of edge pixel at the center of T-junction,  $(x_1, y_1)$ ,  $(x_2, y_2)$ ,  $(x_3, y_3)$  are coordinate of edge pixels at each designated positions. The distance and angles are calculated as follows:

$$l = \sqrt{(x_n - x_m)^2 + (y_n - y_m)^2} \quad (6)$$

where  $l$  is the distance between coordinate  $(x_m, y_m)$  and  $(x_n, y_n)$ .

$$\theta_1 = \cos^{-1}\left(\frac{a^2 + b^2 - d_1^2}{2ab}\right) \quad (7)$$

$$\theta_2 = \cos^{-1}\left(\frac{b^2 + c^2 - d_2^2}{2bc}\right) \quad (8)$$

where  $a, b, c, d_1, d_2$  are distance,  $\theta_1, \theta_2$  are the angles of T-junction as shown in Fig.12. Notice that the coordinate

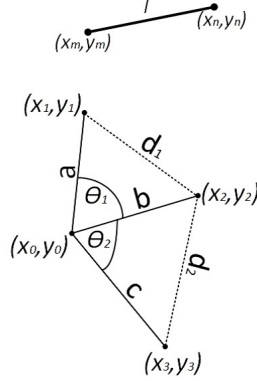


Fig. 12 A diagram of angles of T-junction

of designated pixels can be selected arbitrarily by using square patch as shown in Fig. 13. Due to the variation of edge segments, several positions of the same edge should be used in the computation. The  $11 \times 11$ ,  $17 \times 17$ ,  $25 \times 25$ ,  $31 \times 31$  patches are selected to use in our work. The pixel which is

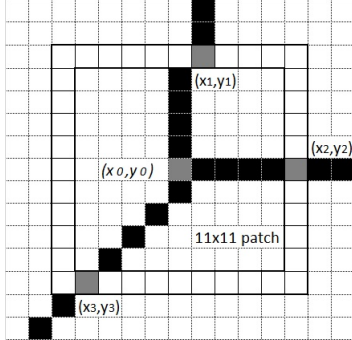


Fig. 13 Illustration of pixels finding using square patch

on the top boundary of the patch will be named as  $(x_1, y_1)$ . The pixel which is on the most left or right boundary of the patch will be named as  $(x_2, y_2)$ . And the pixel which is on the bottom boundary of the patch will be named as  $(x_3, y_3)$ . The distance between pixels can be easily computed by using (6). While  $\theta_1$  and  $\theta_2$  can be computed using (7) and (8). The results of T-junction computation in the image is shown in Table I. Where patch No.1 is  $11 \times 11$ , patch No.2 is  $17 \times 17$ , patch No.3 is  $25 \times 25$ , and patch No.4 is  $31 \times 31$ .

2) *Initial and end points analysis:* In case of the straight weld seam in lap joint welding, the front-view image captured has a unique geometry. That is the initial and end points of the weld seam will be formed as T-junctions in the edge image.

TABLE I The coordinates and angles of T-junctions

Junction No. (coordinate)	$\theta_1$ $\theta_2$	Computed angles using patch No.				Average Angles
		1	2	3	4	
1 (112,527)	$\theta_1$	59	57	59	59	58.50
	$\theta_2$	111	97	94	90	98.00
2 (114,55)	$\theta_1$	90	90	90	86	89.50
	$\theta_2$	111	104	99	97	102.75
3 (130,527)	$\theta_1$	90	97	99	118	95.75
	$\theta_2$	111	116	116	86	115.25
4 (131,53)	$\theta_1$	90	90	90	101	89.00
	$\theta_2$	101	97	99	90	99.50
5 (183,558)	$\theta_1$	68	63	63	61	63.75
	$\theta_2$	78	82	85	82	81.75
6 (187,43)	$\theta_1$	78	82	85	82	81.50
	$\theta_2$	90	90	90	90	90.00

And the angles size formed by intersection of 3 edge lines at T-junctions must be greater than 90 degrees. If the weld seam is a straight line, it is reasonable to assume that the horizontal coordinates of T-junction detected as a candidate of initial and end points should not be located at a different coordinate. However, edge segmentation process normally produces false edges pixels. Thus, in practice, the minimum value of  $\theta_1$  and  $\theta_2$  can be set between 87 degrees and 93 degrees. And the number of different pixels can be set between 0 and 3 pixels. We use 2 aspects as mentioned above to assess T-junction in the image. The flow chart in Fig. 14 shows the decision procedures of initial and end points.

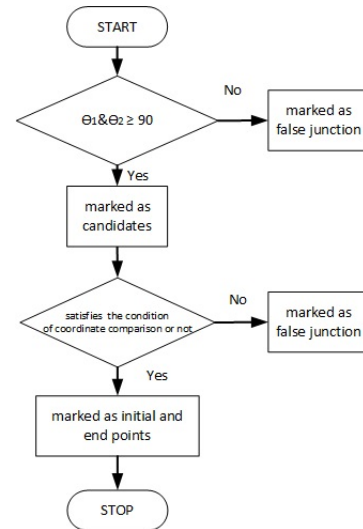


Fig. 14 The flow chart of initial and end points decision

## V. EXPERIMENTAL ENVIRONMENT AND RESULTS

In our study, we use digital monochrome camera, DH-HV3151UC-M, to capture the lap joint image. The size of the image is  $590 \times 312$  pixels. Image processing program are written in C++ language on visual studio 2013 platform. In table II the parameter values used in the experiments are shown.



TABLE II The parameter values in the experiments

Parameter	Value
Standard deviation of Gaussian filter( $\sigma$ )	1.4
T-high, T-low of Canny operator	40,35
Slope threshold for line points grouping( $st$ )	0.5
Minimum value of $\theta_1, \theta_2$	88
The number of different pixels	3

The angle data in table I clearly shows that T-junction No.1, 5, and 6 are not the initial or end points of weld seam because one or both of their angle size is smaller than 88 degrees. And T-junction No.3 will be immediately recognized as initial or end points of weld seam of the lap joint. In our experiment, we usually label the first detected point as the initial point. However, when we focus on the angles of T-junction No.2 and T-junction No.4, we found that they are greater than 88 degrees. Now, the second aspect of initial and end points will be applied to these T-junctions. We set the horizontal coordinate of T-junction No.3 as reference coordinate. As to the results of calculation, the difference of pixels between T-junctions No.3 and 2 is 7 and the difference of pixels between T-junctions No.3 and 4 is 1. Now, we can conclude that T-junction No.4 is the end point of weld seam of lap joint. Fig. 15 shows the result of the process in edge image. In Fig. 16, we mark the detected initial and end points into the original image. This result verify that the proposed method is applicable and suitable for recognizing the initial end points of lap joint welding.

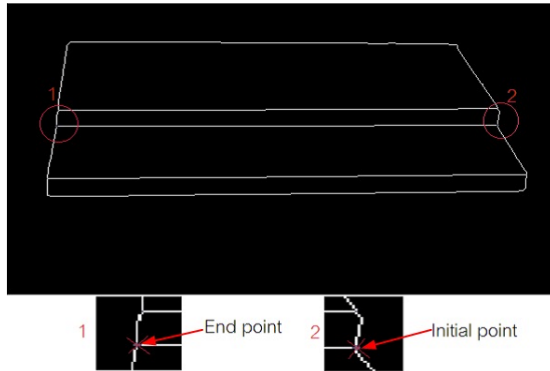


Fig. 15 The result of the initial and end points detection

## VI. CONCLUSION AND FUTURE WORK

The experimental results verify that the proposed image processing techniques can be used to recognize the initial and end points of the weld seam of lap joint. The techniques applied in this work are simple and effective. However, in this study, there are many parameters to be assigned. This will lead to the lack of flexibility. Thus, in the future, the optimization of parameters will be firstly taken into account. Then various forms of lap joints will be tested in order to testify the validity of this method. Furthermore, this method



Fig. 16 The initial and end points in the original image

is expected to be implemented in welding robot system to detect initial and end points of lap joints.

## ACKNOWLEDGMENT

This work was supported by the National Natural Science Foundation of China under Grant 61305024, Grant 6137337, Grant 61227804. And partly supported by Guangdong Natural Science Foundation under Grant S2012010010265.

## REFERENCES

- [1] Gunnar Bolmsjo, Magus Olsson, and Per Cederberg "Robotic arc welding-trens and developments for higher autonomy," Department of Mechanical Engineering,Lund University, 2001.
- [2] Zaojun Fang, De Xu, Min Tan, "Vision-based initail weld point positioning using the geometric relationship between two seams," International Journal of Advanced Manufacturing Technology, 66:1535-1543, 2013.
- [3] WEI Shang-chun, WANG Jian, LIN Tao, CHEN Shan-ben, "Application of image morphology in detecting and extracting the initial welding position," Journal of Shanghai Jiatong University(Science), 617(3):323-326, 2012.
- [4] M.Kong, F.H.Shi, S.B Chen, and T.Lin, "Recognition of the initial position of weld based on the corner detection for welding robot in global environment," Robotic Welding, Intelligent and Automation,LNCIS362, pp.249-255, 2007.
- [5] Xizhang Chen, Shanben Chen, Tao Lin, Yucheng Lei, "Practical method to locate the initial weld position using visual technology," International Journal of Advanced Manufacturing Technology, 30:663-668, 2006.
- [6] Soble I., "An isotropic 3x3 gradient operator," Machine Vision for Three Dimensional Scences, Academic Press, 1990.
- [7] Rafael G. Gonzalez, Richard E. Woods, "Digital image processing", Beijing,Publishing House of Electronics Industry, pp 585-586, 2002.
- [8] Frank Y. Shin, "Image processing and pattern recognition," Fundamentals and techniques, Jonh Wiley&Sons, pp 137-138, 2010.